Proceedings of DETC'98
1998 ASME Design Engineering Technical Conferences
September 13-16, 1998, Atlanta, GA

DETC98/MECH-5914

AN INVESTIGATION INTO COMPLIANT BISTABLE MECHANISMS

Patrick G. Opdahl
Intel Corporation
M/S CH5-263
5000 W. Chandler Blvd.
Chandler, AZ 85226
patrick.g.opdahl@intel.com

Brian D. Jensen
Mechanical Engineering Dept.
Brigham Young University
Provo, Utah 84602
jensenb@et.byu.edu

Larry L. Howell
Mechanical Engineering Dept.
Brigham Young University
Provo, Utah 84602
lhowell@et.byu.edu

ABSTRACT

This paper proposes a new class of bistable mechanisms: compliant bistable mechanisms. These mechanisms gain their bistable behavior from the energy stored in the flexible segments which deflect to allow mechanism motion. This approach integrates desired mechanism motion and energy storage to create bistable mechanisms with dramatically reduced part count compared to traditional mechanisms incorporating rigid links, joints, and springs. This paper briefly reviews bistable mechanism theory, introduces some additional bistable mechanism characteristics, and integrates this theory with compliant mechanism theory. The resulting theory of bistable compliant mechanisms is validated by measuring the force and motion characteristics of several test mechanisms and comparing them to predicted values.

INTRODUCTION

A bistable mechanism has two stable equilibrium positions within its range of motion. It achieves this behavior by storing energy during part of its motion, and then releasing it as the mechanism moves toward a second stable state. Compliant mechanisms, which gain motion through the deflection of their members, offer an economical way to accomplish bistable behavior. Because flexible segments store energy as they deflect, a compliant mechanism can use the same segments to gain both motion and two stable states, allowing a significant reduction in part count. This paper discusses the theory which explains bistable mechanism behavior, introduces compliant bistable mechanisms, and validates the integration of compliant mechanism theory with bistable mechanism theory.

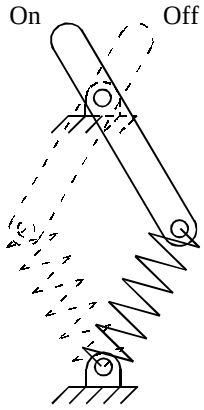

Figure 1: A bistable light switch mechanism. The spring forces the mechanism into either the "on" or "off" position.

Bistable mechanisms have been used as switches, closures, hinges, or other devices where two stable positions are desired. In particular, bistable mechanisms offer two distinct, repeatable stable positions, allowing these devices to require no power input to keep them in each position. Specific energy storage characteristics are necessary in these mechanisms to obtain the bistable behavior. For example, the light switch mechanism shown in Fig. 1 uses a linear spring to keep the mechanism in its "on" or "off" position.

Several writers have discussed the qualities and applica-

tions of bistable mechanisms. Schulze (1955) derived equations for the design of snap-action toggles like the one shown in Fig. 1. His equations maximized the force required to switch the device for a given area the mechanism occupies. Ginsberg and Genin (1984) described the theory of stability and presented a few examples of bistable mechanisms. Artobolevsky (1975), Jensen (1991), and Chironis (1991) also presented several examples of bistable mechanisms. In addition, reliability theory was applied to the design of a bistable mechanism by Howell et al. (1994). A planar two-spring system with two stable positions was also investigated by Pigoski and Duffy (1995). Various examples of bistable MEMS have also been presented (Hälg, 1990; Matoba et al., 1994; Wagner et al., 1996).

Another class of mechanisms, compliant mechanisms, gain some or all of their motion from the deflection of parts of the mechanism. Compliant mechanisms offer several advantages over more traditional rigid-body mechanisms. For example, compliant segments have no friction, noise, or backlash, and they significantly reduce the total part count of the mechanism (Sevak and McLarnan, 1974). Many compliant mechanisms can even be made from one piece of material which bends to achieve desired motion. In addition, previous work has shown that compliant mechanisms can easily be designed and analyzed using the pseudo-rigid-body model, which models compliant segments as one or more rigid segments and rigid-body joints (Howell and Midha, 1994a; Howell and Midha, 1995). Of course, compliance also introduces several challenges. Compliant members have only limited motion, and their deflection requires energy input, reducing the energy which a mechanism can output.

Although many examples of rigid-body bistable mechanisms exist, compliance offers a particularly efficient way to achieve bistable behavior. As mentioned above, flexible members store energy as they deflect. In the proper mechanism configuration, a compliant segment can provide the energy needed to keep the mechanism in its two stable positions. Thus, a compliant bistable mechanism integrates the joint which allows motion and the spring which allows energy storage into one element. This paper defines some of the basic concepts in bistable mechanism theory and integrates them with compliant mechanism theory for the analysis of compliant bistable mechanisms.

A BRIEF REVIEW OF THE PSEUDO-RIGID-BODY MODEL

The motion of many compliant segments can be predicted using standard small-deflection force-deflection equations. However, many compliant segments undergo comparatively large deflections. The closed-form solution for the large deflection of a beam typically involves the evaluation of elliptic integrals, with a separate evaluation required for each loading condition (Frisch-Fay, 1962). This complex process can be avoided by using the pseudo-rigid-body model. This model allows many different types of compliant segments to be analyzed as two or more rigid links joined by pin joints. Torsional springs are placed at the pin joints to model the segment's stiffness. The lengths of the rigid segments, placement of the pin joints, and the spring constants of the torsional springs may all be calculated using various model parameters. While the model is very useful for the analysis of compliant mechanisms, its true power lies in the capability it gives for designing original compliant mechanisms (Jensen et al., 1997). A complete description of the model may be found elsewhere (Howell and Midha, 1994a; Howell and Midha, 1995; Howell and Midha, 1996; Howell et al., 1996).

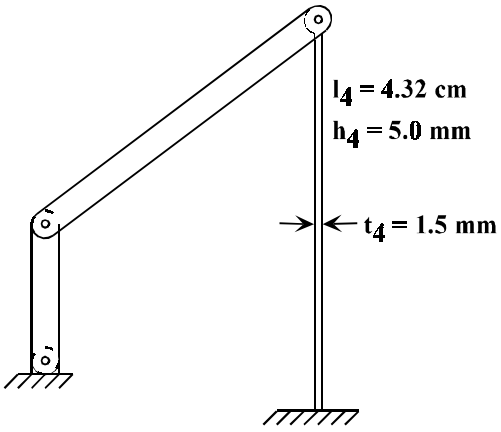

Figure 2: A partially-compliant bistable mechanism. The compliant segment acts as the fourth link of a four-bar mechanism.

As an example, consider the compliant mechanism shown in Fig. 2. Traditional rigid-body kinematics would classify this device as a structure. Only the flexibility of the compliant segment allows it to move as a mechanism. This segment has a length of 4.32 cm, an in-plane thickness of 1.5 mm, and an out-of-plane height of 5.0 mm. The material of the compliant link is polypropylene, with $E = 1.38 \times 10^9$ Pa. The pseudo-rigid-body model may be used to create a rigid-body equivalent mechanism; that is, a mechanism with approximately the same force and motion characteristics as the original compliant mechanism. This pseudo-rigid-body mechanism is shown in Fig. 3. In this mechanism, the compliant segment has been replaced by two rigid segments joined by a pin joint. The model gives the length of the resulting mechanism link as 3.68 cm, and the spring constant of the torsional spring is 0.101 N-m. This mechanism will be analyzed later in the paper to demonstrate compliant bistable mechanism theory. The pseudo-rigid-body model may then be analyzed using the principles of kinematics. This illustrates another advantage of the pseudo-rigid-body model concept: the ability to analyze compliant mechanisms with traditional rigid-body kinematics.

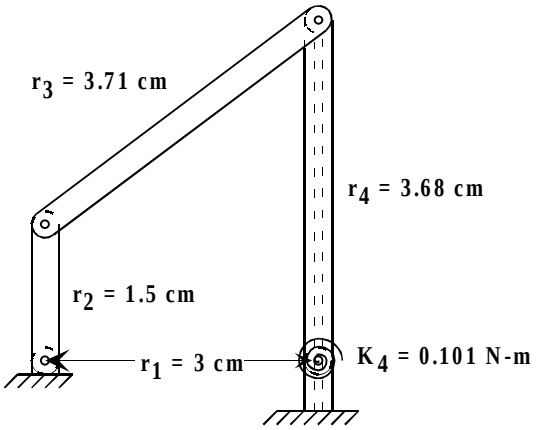

Figure 3: The pseudo-rigid-body model of the mechanism shown in Fig. 2. The length of the pseudo-rigid joint and the value of the spring constant on the torsional spring are found using the pseudo-rigid-body model.

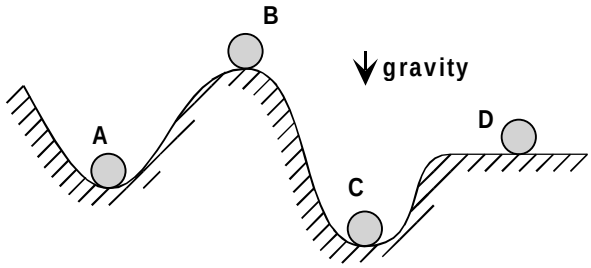

Figure 4: An illustration of the "ball-on-the-hill" analogy. Positions A and C are stable equilibrium positions. Position B is an unstable equilibrium position. Position D is neutrally stable.

THE KEY CONCEPTS IN MECHANISM STABILITY

This section presents the basic theory behind bistable mechanisms. It defines mechanism stability, derives equations for determining the stability of four-bar and crank-slider mechanisms, and proposes key characteristics of bistable mechanisms. The methods and concepts presented in this section will be demonstrated with a compliant bistable mechanism example in the following section.

A Definition of Stability

Several different definitions of stability exist, depending on the application (Leipholz, 1970). The definition presented here comes from the theory of elastic stability of structures (Timoshenko and Young, 1951; Timoshenko, 1961; Simitses, 1976; Ginsberg and Genin, 1984). When a system is in a state of equilibrium, whether loaded or unloaded, "if . . . 'small' external disturbances are applied and the structure reacts by simply performing oscillations about the . . . equilibrium state, the equilibrium is said to be *stable"* (Simitses, 1976). However, if the small external disturbances cause the system to diverge from its equilibrium state, then the equilibrium position is *unstable*. If, on the other hand, the system reacts to the disturbances and stays in the disturbed position, then the equilibrium position is *neutral*. For each of these definitions, the external disturbances may be as small as desired (Simitses, 1976).

The stability of a system may be illustrated using the well-known "ball-on-the-hill" analogy. This analogy is illustrated in Fig. 4. Position A is a stable equilibrium position. If it is shifted from this position by a small amount, it will tend to return to position A or oscillate around it. However, position B is an unstable equilibrium position. Although the ball will stay in this position if placed precisely on top of the hill, it will move to a different position if any disturbance occurs. Position C is stable, while position D is neutrally stable.

The ball-on-the-hill analogy illustrates another important concept in bistable mechanisms. As the ball moves from position A toward position B, the vertical force required to move the ball will increase directly as the slope of the hill increases. At the hill's inflection point, where its slope is greatest, the ball will require the maximum force to continue its motion. Further motion past this point will require decreasing force until the ball is in equilibrium at position B. A very small perturbation in the direction of position C will then cause the ball to move very quickly into this second stable position. This rapid response is often called "snapping." Thus, in a bistable system, when the unstable position is reached, a very small input will cause the system to snap into its second stable position.

Several methods have been developed to determine the stability of a system. Ziegler (1956) described four different, related methods for determining structural stability. In this paper, the energy method will be used. This method is based on the Lagrange-Dirichlet theorem, which states that "when the potential energy . . . has a minimum for an equilibrium position, the equilibrium position is stable" (Leipholz, 1970; Lagrange, 1788). Therefore, to establish the stability of a mechanism, the potential energy of the mechanism must be plotted over the mechanism's motion. Any local minima represent stable positions. The next section shows how this may be done for an arbitrary compliant mechanism whose pseudo-rigid-body model resembles a four-bar mechanism. The equations for finding the potential energy of an arbitrary slider-crank mechanism are also presented.

Potential Energy and Moment Equations for a Pseudo-Rigid-Body Four-Bar Mechanism

Figure 5 shows a pseudo-rigid-body model of a compliant mechanism with arbitrary link lengths and angles. The pseudo-rigid-body model resembles a four-bar mechanism. A moment

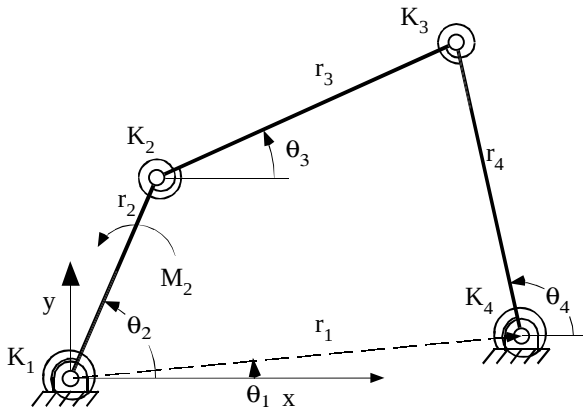

Figure 5: A pseudo-rigid-body model of an arbitrary compliant mechanism which behaves as a four-bar mechanism. Torsional springs at each joint simulate the effects of compliant segments. For purpose of the discussion, link two is the input link.

acts on link two, the input link. A torsional spring at each of the four pin joints allows energy to be stored as the mechanism moves. The torsional springs represent the stiffness of a compliant segment, as specified in the pseudo-rigid-body model. The energy stored in each spring may be found from

$$V_i = \frac{1}{2} K_i \psi_i^2 \tag{1}$$

where V is the potential energy, K is the torsional spring constant, and ψ is the angular deflection of each torsional spring. For each spring shown in the figure,

$$\begin{aligned} \psi_1 &= \theta_2 - \theta_{20} \\ \psi_2 &= (\theta_2 - \theta_{20}) - (\theta_3 - \theta_{30}) \\ \psi_3 &= (\theta_4 - \theta_{40}) - (\theta_3 - \theta_{30}) \\ \psi_4 &= \theta_4 - \theta_{40} \end{aligned} \tag{2}$$

where the "0" subscript symbolizes the initial (undeflected) value of the angle (Howell and Midha, 1994b). The total potential energy of the system may then be given as

$$V = \frac{1}{2}(K_1\psi_1^2 + K_2\psi_2^2 + K_3\psi_3^2 + K_4\psi_4^2) \tag{3}$$

The values of each ψ may be found using kinematic analysis for all positions of the mechanism, allowing a graph of potential energy to be constructed. Any positions corresponding to local minima are stable positions; any local maxima represent unstable equilibrium positions.

The stability of the mechanism can also be determined analytically. The principle of virtual work can be used to find the values of arbitrary moments or forces required to keep a mechanism in a particular position (Howell and Midha, 1994b). For analyzing the bistable characteristics of the mechanism, however, only the value of M_2, as shown in Fig. 5, is necessary. This moment represents the moment that must be applied to the input link to keep the mechanism in a given position. At the equilibrium positions, its value will be zero. The M_2 curve may be found by realizing that it is the first derivative of the energy curve with respect to the angle of the input link. This may be proved by considering the equation for work put into the system:

$$V = \int_{\theta_{20}}^{\theta_2} M_2 d\theta \tag{4}$$

by taking the derivative of this equation, it may be seen that

$$\frac{dV}{d\theta_2} = M_2 \tag{5}$$

assuming that the moment at the initial position is zero. Therefore, M_2 is equal to the first derivative of the energy with respect to the angle of the input link. This means that

$$M_2 = K_1\psi_1 + K_2\psi_2\frac{d\psi_2}{d\theta_2} + K_3\psi_3\frac{d\psi_3}{d\theta_2} + K_4\psi_4\frac{d\psi_4}{d\theta_2} \tag{6}$$

The derivatives in Eq. (6) may be evaluated using Eq. (2) and the additional formulas (Paul, 1979; Erdman and Sandor, 1997)

$$\frac{d\theta_3}{d\theta_2} = h_{32} = \frac{r_2\sin(\theta_4 - \theta_2)}{r_3\sin(\theta_3 - \theta_4)} \tag{7}$$

and

$$\frac{d\theta_4}{d\theta_2} = h_{42} = \frac{r_2\sin(\theta_3 - \theta_2)}{r_4\sin(\theta_4 - \theta_3)} \tag{8}$$

As mentioned previously, the value of M_2 will be zero at all equilibrium positions. The stability of the equilibrium position may be determined by considering the sign of the second derivative of the energy curve at that point. The second derivative is

$$\frac{d^2V}{d\theta_2^2} = K_1 + K_2(1 - 2h_{32} + h_{32}^2 - \psi_2 h'_{32}) \quad (9)$$

$$+ K_3[h_{42}^2 - 2h_{42}h_{32} + h_{32}^2 + \psi 3(h'_{42} - h'_{32})]$$

$$+ K_4(h_{42}^2 + \psi_4 h'_{42})$$

where

$$h'_{32} = \frac{dh_{32}}{d\theta_2} = \frac{r_2}{r_3}\left[\frac{\cos(\theta_4 - \theta_2)}{\sin(\theta_3 - \theta_4)}(h_{42} - 1) - \frac{\sin(\theta_4 - \theta_2)\cos(\theta_3 - \theta_4)}{\sin^2(\theta_3 - \theta_4)}(h_{32} - h_{42})\right] \quad (10)$$

and

$$h'_{42} = \frac{dh_{42}}{d\theta_2} = \frac{r_2}{r_4}\left[\frac{\cos(\theta_3 - \theta_2)}{\sin(\theta_4 - \theta_3)}(h_{32} - 1) - \frac{\sin(\theta_3 - \theta_2)\cos(\theta_3 - \theta_4)}{\sin^2(\theta_4 - \theta_3)}(h_{32} - h_{42})\right] \quad (11)$$

When the value of M_2 is zero, the equilibrium position will be stable if the second derivative of potential energy is positive. If the second derivative of potential energy is negative, the equilibrium position is unstable, and if it is zero, the equilibrium position is neutrally stable.

As the mechanism moves from one stable position to another, the absolute value of M_2 will increase to some maximum before decreasing down to zero at the unstable position. This maximum moment represents the largest moment that must be applied to the input link to make the mechanism snap into its second position. This important value may be called the "critical moment," or, if a force is applied instead, the "critical force."

In addition, a high value of the second derivative at a stable position means that the energy curve is changing very rapidly at that point. This means that the restoring force returning the mechanism to that position is relatively high. Thus, the value of the second derivative at a stable position may be called the stable position's "stiffness," where a high stiffness corresponds to a rapidly increasing restoring force.

Potential Energy and Moment Equations for a Slider-Crank Mechanism

Figure 6 shows an arbitrary slider-crank mechanism, with springs placed to represent compliant segments. The potential energy of this system may also be found from

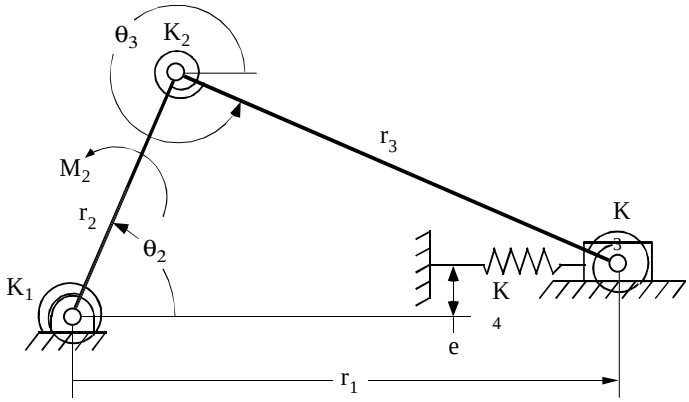

Figure 6: A pseudo-rigid-body model of an arbitrary compliant mechanism which behaves as a slider-crank mechanism. Torsional springs at the revolute joints, as well as the linear spring attached to the slider, represent compliant segments.

$$V = \frac{1}{2}(K_1\psi_1^2 + K_2\psi_2^2 + K_3\psi_3^2 + K_4\psi_4^2) \quad (12)$$

In this case,

$$\begin{aligned} \psi_1 &= \theta_2 - \theta_{20} \\ \psi_2 &= (\theta_2 - \theta_{20}) - (\theta_3 - \theta_{30}) \\ \psi_3 &= \theta_3 - \theta_{30} \\ \psi_4 &= r_1 - r_{10} \end{aligned} \quad (13)$$

where r_1 is defined in Fig. 6 (Howell and Midha, 1994b). The values of the various angles may be found for each position of the mechanism using kinematic analysis. The moment M_2 required to keep the mechanism in position can also be found, using θ_2 as the generalized coordinate, as

$$M_2 = K_1\psi_1 + K_2\psi_2\frac{d\psi_2}{d\theta_2} + K_3\psi_3\frac{d\psi_3}{d\theta_2} + K_4\psi_4\frac{d\psi_4}{d\theta_2} \quad (14)$$

Evaluation of the derivatives in Eq. (14) requires the formulas (Howell and Midha, 1994b)

$$\frac{d\theta_3}{d\theta_2} = g_{32} = -\frac{r_2\cos\theta_2}{r_3\cos\theta_3} \quad (15)$$

and

$$\frac{dr_1}{d\theta_2} = g_{12} = -\frac{r_2 \sin(\theta_2 - \theta_3)}{\cos\theta_3} \tag{16}$$

Finally, the second derivative of the potential energy may be found from

$$\frac{d^2V}{d\theta_2^2} = K_1 + K_2(1 - 2g_{32} + g_{32}^2 - \psi_2 g'_{32}) \tag{17}$$

$$+ K_3(g_{32}^2 + \psi 3 g'_{32}) + K_4(g_{12}^2 + \psi_4 g'_{12})$$

where

$$g'_{32} = \frac{d^2\theta_3}{d\theta_2^2} = \frac{r_2}{r_3}\left(\frac{\sin\theta_2}{\cos\theta_3} - \frac{\cos\theta_2 \tan\theta_3}{\cos\theta_3} g_{32}\right) \tag{18}$$

and

$$g'_{12} = \frac{d^2 r_1}{d\theta_2^2} = -r_2\cos\theta_2 - r_3 g_{32}^2 \cos\theta_3 - r_3 g'_{32} \sin\theta_3 \tag{19}$$

These equations will allow the analysis of the energy states of a slider-crank mechanism.

A Summary of Bistable Mechanism Behavior

The key bistable mechanism characteristics may be summarized with the following statements:

- A mechanism will have a stable equilibrium position when the first derivative of the potential energy curve is zero and the second derivative of the potential energy curve is positive.
- A mechanism will have an unstable equilibrium position when the first derivative of the potential energy curve is zero and the second derivative of the potential energy curve is negative.
- A mechanism will have a neutrally stable equilibrium position when the first derivative of the potential energy curve is zero and the second derivative of the potential energy curve is also zero.
- Because two local minima must always contain one local maximum between them, an unstable or neutrally stable position will always occur between any two stable states.
- The critical moment (the maximum load required for the mechanism to change stable states) may be found by evaluating the moment curve when the second derivative of potential energy is zero.

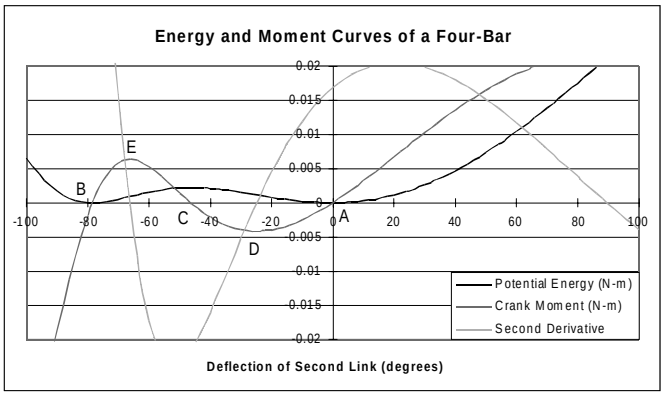

Figure 7: The energy and crank moment curves for the mechanism shown in Fig. 2. The second derivative of energy is also shown.

- The stiffness of a stable equilibrium position is equal to the value of the second derivative of potential energy at that position.

These statements are all demonstrated in the following example.

A COMPLIANT BISTABLE MECHANISM EXAMPLE

In the mechanism shown in Fig. 2, the compliant segment oscillates as the crank turns. Because the compliant link is undeflected for two different crank positions, this mechanism is bistable. As explained previously, its pseudo-rigid-body model is shown in Fig. 3. For the purpose of this analysis, θ_2 is defined as the crank angle, shown in Fig. 5, and $\Delta\theta_2$ is defined as the change in crank angle, or $\theta_2 - \theta_{20}$, where θ_{20} is the initial crank angle.

Using the mechanism shown in Fig. 3, the potential energy and crank torque curves may be calculated using the methods outlined in the preceding section. The values of ψ_1, ψ_2, ψ_3, and ψ_4 all come from kinematic analysis, while $K_1 = K_2 = K_3 = 0$. K_4 is given by the pseudo-rigid-body model (see Fig. 3) as 0.101 N-m. Equations (3) through (11) may be evaluated for any range of θ_2. The resulting curves for potential energy, crank moment, and second derivative of potential energy as a function of θ_2 are shown in Fig. 7.

These curves show that the mechanism will be stable when $\Delta\theta_2 = 0°$, corresponding to position A in Fig. 7, and when $\Delta\theta_2 = -79°$, corresponding to position B. The mechanism is shown in the second stable equilibrium position in Fig. 8. The mechanism also has an unstable position at $\Delta\theta_2 = -45°$, corresponding to position C in Fig. 7. When moving from position A to position B, the critical moment is about 0.004 N-m, as shown at D in Fig. 7. When moving from position B to position A, the critical moment is about 0.0065 N-m, as shown at E.

This mechanism has two unstable equilibrium positions and two stable equilibrium positions. However, the energy stored in

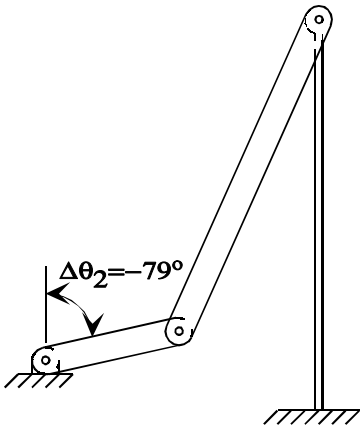

Figure 8: The mechanism shown in Fig. 2 in its second stable position.

the unstable position at $\Delta\theta_2 = -45°$ is much lower than the energy stored at the other unstable position. This is because the compliant segment has a much smaller deflection at this unstable equilibrium condition. For this reason, the mechanism would most likely be actuated by turning the crank clockwise from the first position, shown in Fig. 2, into the second stable position shown in Fig. 8.

The stiffness of the stable positions may also be found from Eq. (9). When $\Delta\theta_2 = 0°$, the value of the second derivative of energy is 0.017 N-m/rad. At $\Delta\theta_2 = -79°$, the stiffness is 0.068 N-m/rad. This means that the instantaneous slope of the moment curve is four times higher at the second stable position, indicating that the equivalent restoring moment at the input link will be about four times higher if the mechanism is perturbed in this position. Note that this does not relate to the critical moment required to cause the mechanism to snap into its other position. Rather, it expresses the rate at which the restoring moment initially increases.

EXPERIMENTAL VALIDATION

The example presented above and the method used to solve it depend on accurate modeling of compliant bistable mechanisms. To test the predictions of the pseudo-rigid-body model for bistable mechanisms, several test mechanisms were designed and fabricated. The model is accurate if it successfully predicts the force required to create a given deflection in the bistable mechanism. Therefore, the motion of each mechanism and the force required to produce that motion were measured and compared to the predictions of the pseudo-rigid-body model and finite element analysis. Three basic types of test mechanisms were used, as shown in Fig. 9. Each of these mechanisms has two stable positions.

For testing, each mechanism was milled out of quarter-inch polypropylene using a three-axis mill. Each mechanism was then placed on a breadboard, and potentiometers were used to measure the mechanisms' motion while a force meter measured the force required to actuate each mechanism. For all cases, three measurements were made of the force-deflection data of the mechanism, and the three results were averaged. The force-deflection results were compared to the predictions of finite element analysis and the pseudo-rigid-body model.

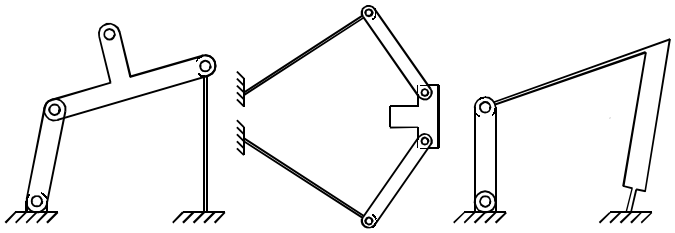

Figure 9: The three test mechanisms. The pseudo-rigid-body models of the three mechanisms are shown in Fig. 10.

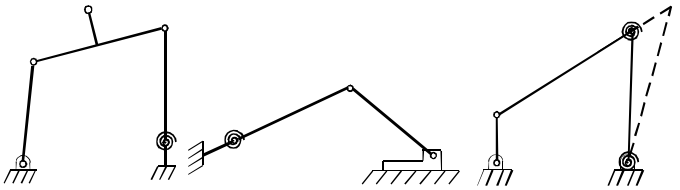

Figure 10: The pseudo-rigid-body models of the three test mechanisms.

The pseudo-rigid-body model of each mechanism is shown in Fig. 10. Mechanisms A and C are modeled by four-bar mechanisms, while mechanism B is modeled by a crank-slider mechanism. These models were used to analyze each mechanism using the methods outlined in the preceding sections. This process will be explained in more detail for each mechanism.

Mechanism A

Four different configurations of mechanism A were tested. Table 1 shows the dimensions of each variation, where the dimensions are defined in Fig. 11. The differences among the four mechanisms are the length of the input link and the thickness of the compliant segment. Each of these four mechanisms was tested by pushing or pulling the coupler point, point P, and recording its motion and the force required to keep the mechanism in each position. The position and force were measured in five degree increments of the crank angle over the range of motion between the two stable positions. Figure 12 shows the results for mechanism A2, and the results for the

Table 1: The dimensions of the variations of Mechanism 1.

	Mech. A1	Mech. A2	Mech. A3	Mech. A4
r_1, cm	11.3	11.3	11.3	11.3
r_2, cm	7.6	7.6	5.9	5.9
r_3, cm	11.5	11.5	11.5	11.5
L_4, cm	10.8	10.8	10.8	10.8
t_4, cm	0.19	0.24	0.19	0.24
a_3, cm	5.7	5.7	5.7	5.7
b_3, cm	5.6	5.6	5.6	5.6

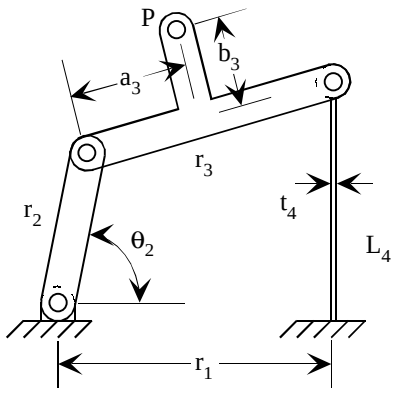

Figure 11: The dimensions of mechanism A.

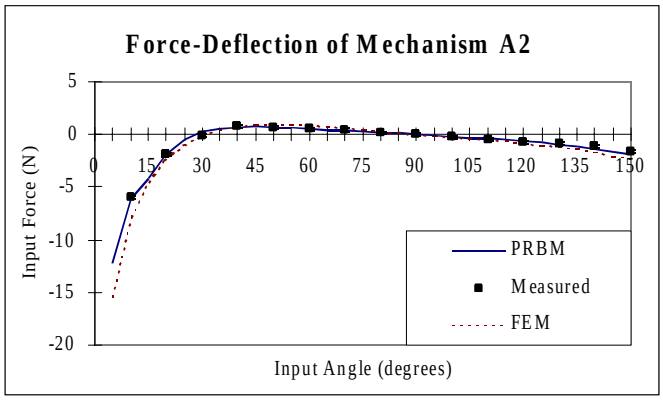

Figure 12: The input force on the coupler point required to keep mechanism A2 in position.

other three mechanism variations are similar. Full results for all test mechanism variations are reported by Opdahl (1996). As

Table 2: Comparison of the measured critical force with the predicted values. All values are in Newtons.

	PRBM	FEA	Measured
Mech A1	0.34	0.32	0.33
Mech A2	0.74	0.97	0.76
Mech A3	0.46	0.44	0.42
Mech A4	0.99	0.98	0.85

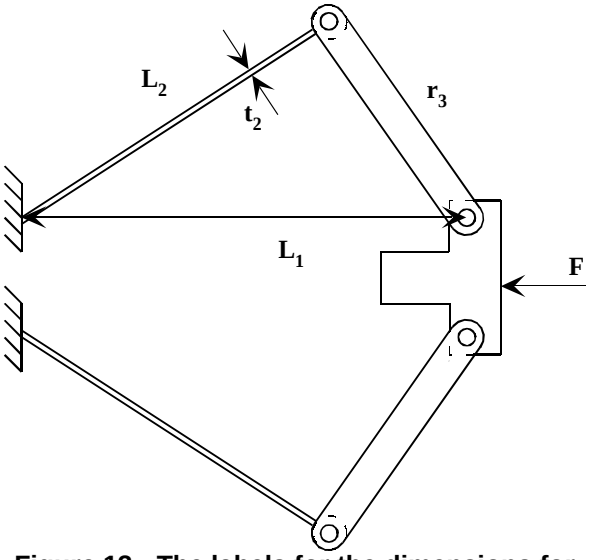

Figure 13: The labels for the dimensions for mechanism B.

the graph shows, the pseudo-rigid-body model accurately predicted the mechanism's movement in response to an input force. The error in the measurements is ±0.15 N. The results of the finite element modeling also lie along the predictions of the model.

Table 2 compares the critical force of each mechanism variation as measured, predicted by the model, and predicted by finite element analysis. The data is given for the critical force as the mechanism moves from its first stable position (shown in Fig. 11) to its second stable position. Once again, the two predictions and the measured value correlate very accurately.

Mechanism B

Figure 13 shows the dimensions of mechanism B. Two variations of this mechanism were tested; their dimensions are given in Table 3. The only difference between the two variations is the thickness of the compliant segment. To test these

Table 3: The dimensions of the two variations of mechanism B.

	Mech. B1	Mech. B2
L_1, cm	13.49	13.49
L_2, cm	9.65	9.65
r_3, cm	7.62	7.62
t_2, cm	0.20	0.31

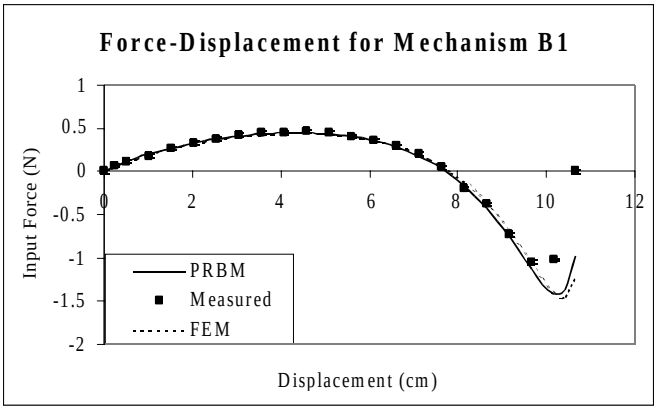

Figure 14: Force-displacement data for mechanism B1.

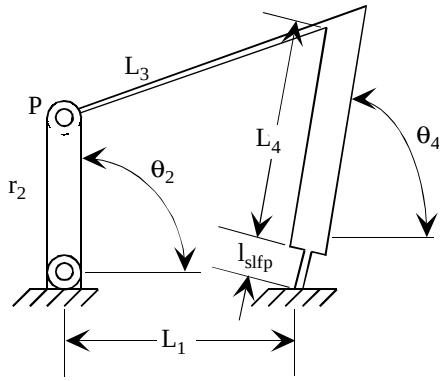

Figure 15: Symbolic dimensions for mechanism C.

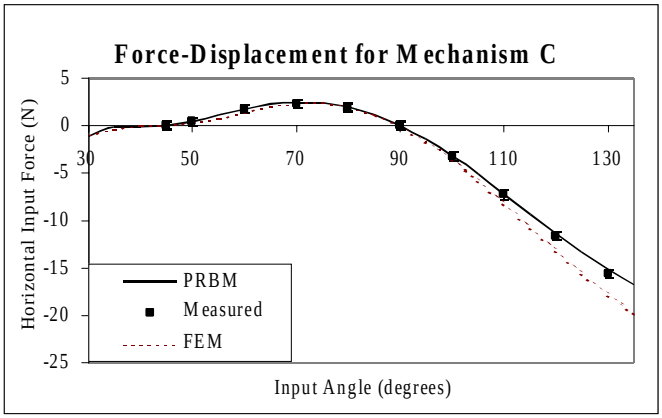

Figure 16: The results of testing for mechanism C.

mechanisms, they were pushed at the location shown by the applied force in Fig. 13. The horizontal displacement of this point and the force required to produce this horizontal displacement were recorded. The force was measured for 0.25 cm increments of horizontal displacement. The result for mechanism B1 is shown in Fig. 14. The measurement error in this figure is also about ±0.15 N. The graph shows that the pseudo-rigid-body model closely predicts the actual force-deflection curve of the mechanism. Results for mechanism B2 are very similar (Opdahl, 1996).

Mechanism C

The dimensions of mechanism C are given symbolically in Fig. 15. The values are: $L_1 = 8.5$ cm, $r_2 = 3.0$ cm, $L_3 = 11.1$ cm , $L_4 = 8.5$ cm, and $l_{slfp} = 0.8$ cm. In addition, $\theta_2 = 90$ degrees and $\theta_4 = 82$ degrees. This mechanism was tested by pushing on the end of link two, labeled point P in the figure. The force required to keep the mechanism in position was recorded for five degree increments of the crank angle. The result is shown in Fig. 16. The measurement error is also about 0.15 N. In addition, the critical force was measured as the mechanism went from the position shown in Fig. 15 to its second stable position. This critical force was found to be 2.3 N. The pseudo-rigid-body model predicted a value of 2.46 N, and finite element analysis predicted 2.38 N. These results show that the pseudo-rigid-body model can be used to design and analyze bistable mechanisms with a good degree of accuracy.

CONCLUSION

Bistable mechanisms provide an excellent way to make switches, relays, closures, and many other useful devices. These mechanisms use a form of energy storage to create two stable positions. Because compliant mechanisms inherently store energy in their flexible members, they are particularly well-suited for bistable mechanisms. The pseudo-rigid-body model allows the modeling of such mechanisms as rigid-body mechanisms whose behavior can be analyzed using rigid-body kinematics. In addition, the torsional spring constants given by the model provide a way to easily incorporate considerations of potential energy into the analysis. By coupling the rigid-body kinematics with calculations of potential energy and the moment required to move a compliant mechanism to a particular position, a mechanism's bistable characteristics can be found.

Specifically, the location of the equilibria, the determination of each equilibrium position's stability, and the maximum force or moment required to snap between two stable states may be found from the equations presented here. This maximum force or moment has been called the "critical force" or "critical moment." The "stiffness" of a stable position has been defined as the second derivative of the potential energy curve at that point.

An example has also been presented to demonstrate the application of this method to the analysis of a compliant bistable mechanism, and the testing of several compliant bistable mechanisms has been reported. The testing established the validity of the use of the pseudo-rigid-body model for bistable mechanism analysis. This result paves the way for future studies into type and dimensional synthesis of compliant bistable mechanisms. This will allow the design of compliant bistable mechanisms with specified stable states and desired critical moments which do not exceed some maximum strength.

ACKNOWLEDGMENTS

The assistance of Scott Lyon is gratefully appreciated. This work is supported under a National Science Foundation Graduate Fellowship and National Science Foundation Career Award No. DMI-9624574.

REFERENCES

Artobolevsky, I.I., 1975, *Mechanisms in Modern Engineering Design*, MIR Publishers, Moscow, Vol. I.

Chironis, N.P., 1991, *Mechanisms and Mechanical Devices Sourcebook*, McGraw-Hill, Inc., New York.

Erdman, A.G. and Sandor, G.N., 1997, *Mechanism Design: Analysis and Synthesis*, Vol. 1, 3rd Ed., Prentice Hall, New Jersey.

Frisch-Fay, R., 1962, *Flexible Bars*, Butterworth, Washington, D.C.

Ginsberg, J.H. and Genin, J, 1984, *Statics and Dynamics, Combined Version*, John Wiley & Sons, New York.

Hälg, B., 1990, "On A Nonvolatile Memory Cell Based on Micro-electro-mechanics," *IEEE Micro Electro Mechanical Systems 1990*, pp. 172-176.

Howell, L.L. and Midha, A., 1994a, "A Method for the Design of Compliant Mechanisms with Small-Length Flexural Pivots," *ASME Journal of Mechanical Design*, Vol. 116, No. 1, pp. 280-290.

Howell, L.L. and Midha, A., 1994b, "The Development of Force-Deflection Relationships for Compliant Mechanisms," *Machine Elements and Machine Dynamics*, DE-Vol. 71, 23rd ASME Biennial Mechanisms Conference, pp. 501-508.

Howell, L.L, Rao, S.S., and Midha, A., 1994, "The Reliability-Based Optimal Design of a Bistable Compliant Mechanism," *ASME Journal of Mechanical Design*, Vol. 117, No. 1, pp. 156-165.

Howell, L.L. and Midha, A., 1995, "Parametric Deflection Approximations for End-Loaded, Large-Deflection Beams in Compliant Mechanisms," *ASME Journal of Mechanical Design*, Vol. 117, No. 1, pp. 156-165.

Howell, L.L. and Midha, A., 1996, "Parametric Deflection Approximations for Initially Curved, Large-Deflection Beams in Compliant Mechanisms," *Proceedings of the 1996 ASME Design Engineering Technical Conferences*, 96-DETC/MECH-1215.

Howell, L.L, Midha, A., and Norton, T.W., 1996, "Evaluation of Equivalent Spring Stiffness for Use in a Pseudo-Rigid-Body Model of Large-Deflection Compliant Mechanisms," *ASME Journal of Mechanical Design*, Vol. 118, No. 1, pp. 126-131.

Jensen, P.W., 1991, *Classical and MOdern Mechanisms for Engineers and Inventors*, Marcel Dekken, Inc., New York.

Jensen, B.D., Howell, L.L., Gunyan, D.B., and Salmon, L.G., 1997, "The Design and Analysis of Compliant MEMS Using the Pseudo-Rigid-Body Model," *Microelectomechanical Systems (MEMS) 1997*, presented at the 1997 ASME International Mechanical Engineering Congress and Exposition, November 16-21, 1997, Dallas, Texas, DSC-Vol. 62, pp. 119-126.

Lagrange, J.L., 1788, *Mecanique Analytique*, Vol. 1, Pt.1, Sec. 3, Art 5, published 1853 by Mallet-Bachelier, Paris.

Leipholz, H., 1970, *Stability Theory*, Academic Press, New York and London.

Matoba, H., Ishikawa, T., Kim, C., and Muller, R.S., 1994, "A Bistable Snapping Mechanism," *IEEE Micro Electro Mechanical Systems 1994*, pp. 45-50.

Opdahl, P.G., 1996, "Modeling and Analysis of Compliant Bi-Stable Mechanisms Using the Pseudo-Rigid-Body Model," M.S. Thesis, Brigham Young University, Provo, Utah.

Paul, B., 1979, *Kinematics and Dynamics of Planar Machinery*, Prentice-Hall, Inc., Englewood Cliffs, New Jersey.

Pigoski, T.M and Duffy, J., 1995, "An Inverse Force Analysis of a Planar Two-Spring System," *Journal of Mechanical Design*, Trans. ASME, Vol. 117, pp. 548-553.

Sevak, N.M., McLarnan, C.W., 1974, "Optimal Synthesis of Flexible Link Mechanisms with Large Static Deflections," ASME Paper No. 74-DET-83.

Schulze, E.F., 1955, "Designing Snap-Action Toggles," *Product Engineering*, November 1955, pp. 168-170.

Simitses, G.J., 1976, *An Introduction to the Elastic Stability of Structures*, Prentice-Hall, Inc., Englewood Cliffs, New Jersey.

Timoshenko, S. and Young, D.H., 1951, *Engineering Mechanics 3rd Ed.*, McGraw-Hill Book Company, Inc., New York.

Timoshenko, S., 1961, *Theory of Elastic Stability, 2nd Ed.*, McGraw-Hill Book Company, Inc., New York.

Wagner, B., Quenzer, H.J., Hoershelmann, S., Lisec, T., and Juerss, M., 1996, "Bistable Microvalve with Pneumatically Coupled Membranes," *Proceedings of IEEE Micro Electro Mechanical Systems 1996*, p. 384-388.

Ziegler, H., 1956, "On the Concept of Elastic Stability," *Advances in Applied Mechanics*, Vol. IV (Ed.: H.L. Dryden and Th. von Karman), Academic Press, Inc., New York, New York.